Parallel-plate avalanche counter (PPAC) detector commissioned for the MDM focal plane

E. Harris,[1,2] G.V. Rogachev,[1,2] G. Chubaryan,[1] H. Jayatissa,[1,2,3] E. Koshchiy,[1] and K. Rao[1,2,4]
[1]*Cyclotron Institute, Texas A&M University, College Station, Texas 77843*
[2]*Department of Physics & Astronomy, Texas A&M University, College Station, Texas 77843*
[3]*Argonne National Laboratory, Lemont, Illinois, 60439*
[4]*Department of Physics & Astronomy, Rice University, Houston, Texas, 77005*

PPACs have played an important role in nuclear science since the recognition of their superior performance as heavy-ion detectors [1, 2]. They exhibit many desirable characteristics such as their simple design, resistance to radiation damage, arbitrary sizing allowing for large solid angles, and straightforward particle identification from position and timing. The commissioning of such a detector for the Texas A&M Cyclotron Institute (CI) began because of the need to measure low-energy heavy ions for future experiments. The primary design criteria were that the detectors should provide a reasonable position resolution to separate ions with similar magnetic rigidities, a high time resolution, and minimal energy loss for heavy ions. A PPAC detector system has since been developed and manufactured at the CI to be used in conjunction with the Multipole-Dipole-Multipole (MDM) spectrometer [3]. TexPPAC will be utilized for experiments with low energy stable beams to constrain reaction rates and other parameters of relevant astrophysical processes. Since its installment on the MDM beamline in September 2020, it has been utilized for several experiments including the measurement of ANCs relevant to the $^{12}C(\alpha,\gamma)^{16}O$ reaction, the determination of branching ratios for the ^{12}C Hoyle state, and the study of alpha decay branches in ^{19}Ne via the $^{21}Ne(p,t)^{19}Ne$ reaction.

TexPPAC consists of two plane-parallel PPAC detectors separated by a variable distance that may be chosen to fit the needs of the experiment. Each PPAC is made of two electrodes on either side of a central biased electrode. The central cathode is made of a 220 $\mu g/cm^2$ Mylar foil with a 80 $\mu g/cm^2$ aluminum coating on both sides. The anodes consist of two PCBs with X- and Y-direction wires made of a Be-Cu alloy with a diameter of 50 μm. There is a 0.635 mm pitch between each wire which spans 40 cm x 10 cm creating the active region of the detector.

The parallel plate geometry allows for a uniform electric field between the electrodes where electron amplification occurs in the quencher gas used to fill the detector chamber. When a particle travels through the detector, it ionizes the gas between the electrodes creating electron-ion pairs. These electrons produced from the primary ions may gain sufficient kinetic energy through acceleration in the strong electric field and cause a subsequent avalanche of electrons known as a Townsend avalanche [4]. Three electrical pulses are produced from this process: two from the X-plane and Y-plane anode wires giving 2D position signals, and one from the central cathode giving the timing signal.

2D position information from the anode wires is obtained by the delay-line readout method. One side of each wire array is connected to a common ground while the other end of each wire in the array is sent to its respective delay line in the X- or Y- direction. All four delay lines were created by wrapping a coated copper wire around a PCB. The X and Y delay lines have a 287 Ω and 214 Ω impedance respectively. The position of the impinging particle is determined by the time difference between the signals that are transmitted to either end of the delay line. By utilizing the fast avalanche electron signals from the anode wires, the detector can handle high beam rates of a few MHz (~ 5×10^6 pps) [4]. Fig. 1 shows components of the fully assembled TexPPAC detector.

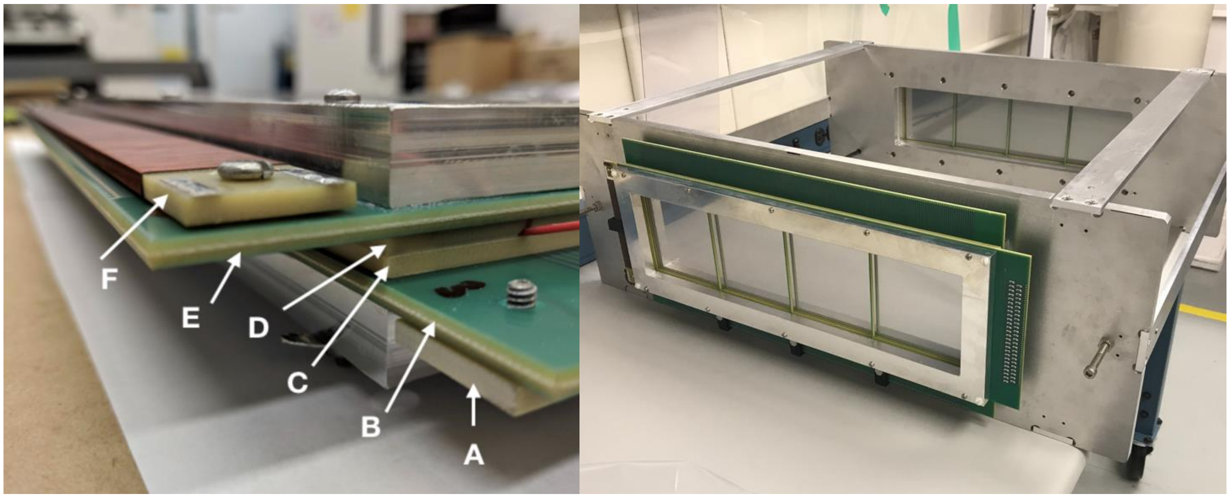

Fig. 1. (a) A picture of the order of the individual components of a PPAC detector. A) Delay line for Y-anode. B) Y-anode. C) PCB with mylar foil glued on top. D) 3mm Spacer. E) X-anode. F) Delay line for X-anode. (b) Fully assembled Tex-PPAC detector on frames.

To reduce the energy loss of the low-energy ions, the TexPPAC detectors were placed in a single gas volume with only one entrance window into the chamber. The entrance window is made of a thin Mylar film of 2 μm thickness. Very low pressures of Pentane gas between 3-8 Torr were used to further decrease interference along the ion path. The stability of the gas pressure was maintained with an inlet needle valve and an outlet scroll pump with a gas flow controller.

In order to investigate the characteristics of the TexPPAC detector, an experiment was performed using a 10 MeV/u beam of ^{20}Ne that was impinged on a ^{97}Au target of 600 μg/cm^2 thickness. With the MDM set to 15 degrees from the beam axis and the detection of scattered ^{20}Ne in TexPPAC, we were able to gather information about the detector specifications and overall performance. The position signals from each delay line and the time signals from each PPAC cathode were amplified by custom-made fast current

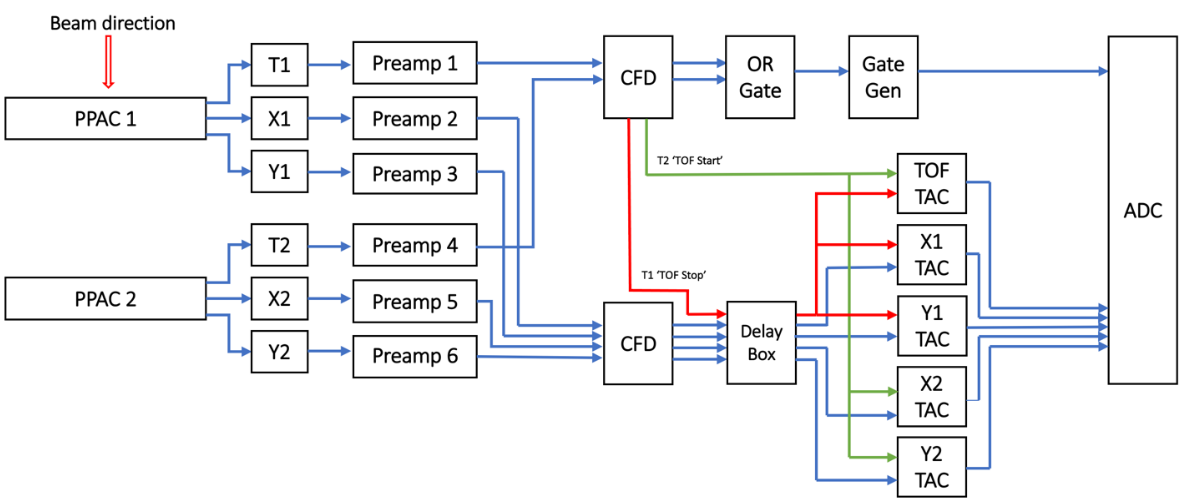

Fig. 2. Electronics and DAQ setup used for TOF, position, and efficiency measurements.

pre-amplifiers. Fig. 2 shows a schematic of the electronics used for the commissioning experiment.

The time resolution was calculated via the ion time-of-flight (TOF) between the cathodes of the two PPAC detectors. Measurements were performed with different gas pressures to find the optimal running conditions and the corresponding time resolutions. The gas pressure was increased from 2-7 Torr in steps of 1 Torr, while the bias voltage was finely tuned for each pressure setting to obtain the highest detection efficiency. Fig. 3(a) shows a typical TOF spectrum where the MDM was set to send ^{20}Ne down the center of TexPPAC, and 3(b) shows the time resolution as a function of gas pressure. It can be seen that the time resolution tends to improve as the gas pressure decreases. The ideal running condition gave a time resolution of 755.8 ps.

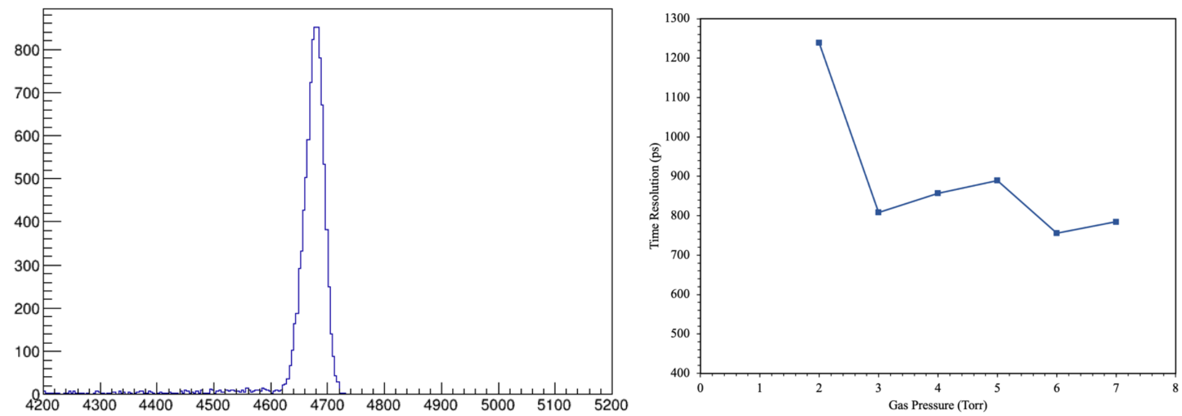

Fig. 3. (a) TOF spectrum for 6 torr of Pentane gas (Y axis in channels). (b) Plot of time resolution as a function of gas pressure.

The setup with the highest time resolution was chosen to characterize the position resolution and efficiency. The position resolution was found by setting the MDM to send scattered beam directly down the center of TexPPAC. As shown in Fig. 1(b), there is a central support column of 2 mm thickness along the active region of the detector. This column can be seen in the X-plane position spectrum of PPAC-1 in Fig. 4(a). Since it is not fully resolved, this indicates the resolution is worse than 2 mm. The ‘5-finger’

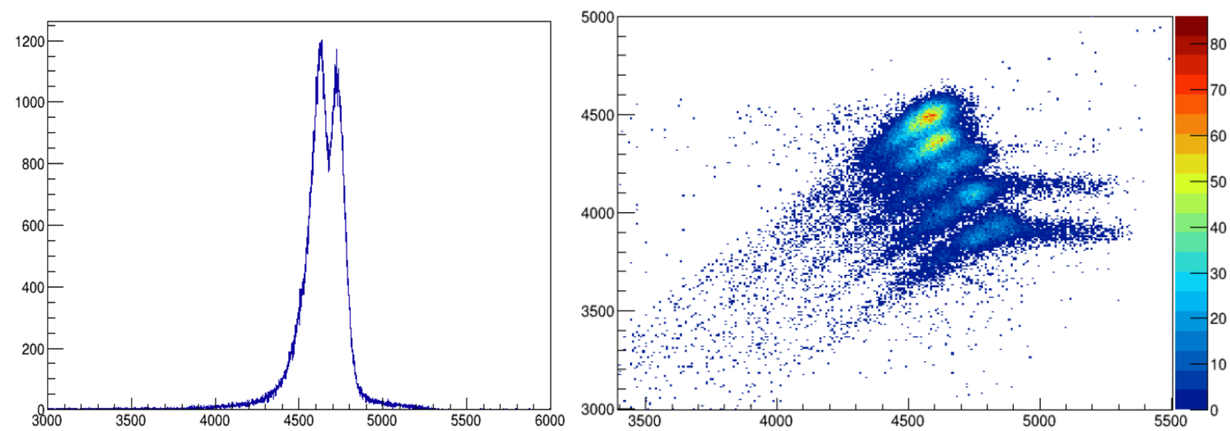

Fig. 4. (a) X position in PPAC-1 showing the effect of the 1 mm central support frame (b) Plot of X2 vs. X1 for the 5-finger mask.

mask located upstream of the MDM was also used to determine the position resolution (Fig 4(b)). The mask has five rectangular slits that are each 11.7 mm high and 1.6 mm wide. They are made of brass with a lead backing to stop particles that don't pass through the slit. A position resolution of 6.0 mm was found for the slits of 1.6 mm width.

To calculate the efficiency of both PPACs, the timing signal of either PPAC-1 or PPAC-2 was used as the trigger for the DAQ system. The detection efficiency of each setup can be calculated by:

$$\varepsilon_1 = \frac{N_1 \& N_2}{N_1} \qquad \varepsilon_2 = \frac{N_1 \& N_2}{N_2} \tag{1}$$

where N_1 and N_2 are the number of events in PPAC-1 and PPAC-2 respectively, and N_1&N_2 is the coincident number of events seen in both PPACs. High efficiencies of ε_1 = 98% and ε_2 = 99% were found.

TexPPAC has been characterized with this commissioning run and will continue to be used for experiments on the MDM beamline. The high timing resolution, reasonable position resolution, and high efficiency allows for reliable particle identification with TOF and position measurements in the MDM focal plane.

[1] J. Christiansen *et al.*, Nucl. Phys. **A239**, 253 (1975).

[2] H. Steltzer, Nucl. Instrum. Methods **133**, 409 (1976).

[3] H. Jayatissa *et al.*, *Progress in Research*, Cyclotron Institute, Texas A&M University, (2018-2019) p. IV-42.

[4] H. Kumagai *et al.*, Nucl. Instrum. Methods Phys. Res. **B317**, 717 (2013).